INSTITUTE OF PHYSICS PUBLISHING MODELLING AND SIMULATION IN MATERIALS SCIENCE AND ENGINEERING

Modelling Simul. Mater. Sci. Eng. **12** (2004) 33–41 PII: S0965-0393(04)67834-X

Possible structures of nonstoichiometric tin oxide: the composition Sn_2O_3

Matti A Mäki-Jaskari[1] **and Tapio T Rantala**

Institute of Physics, Tampere University of Technology, PO Box 692, FIN-33101 Tampere, Finland

E-mail: matti.maki-jaskari@tut.fi

Received 9 March 2003, in final form 22 July 2003
Published 3 November 2003
Online at stacks.iop.org/MSMSE/12/33 (DOI: 10.1088/0965-0393/12/1/004)

Abstract

Structural aspects of crystalline tin oxide and its interfaces with composition Sn_2O_3 are considered computationally based on first principles density functional calculations. The possibility of formation of different nonstoichiometric tin oxide crystals and SnO_2/SnO interfaces is shown. The lowest total energy per Sn_2O_3 unit was evaluated for a layered Sn_2O_3 crystal, where oxygen vacancies are arranged into the (101) plane in a rutile structure system. Interface structures with orientations $SnO_2(101)$/SnO(001) and $SnO_2(100)$/SnO(100), corresponding to composition Sn_2O_3 are only slightly less stable. Their estimated interface energies are $0.15\,J\,m^{-2}$ and $0.8\,J\,m^{-2}$, respectively. All geometries have components similar to well-known rutile structure SnO_2 and litharge structure SnO geometries. Most stable Sn_2O_3 crystals include SnO_6 octahedra similar to those found in rutile structure SnO_2.

1. Introduction

Binary oxides of tin, prepared in many different ways, form a class of widely employed materials due to their important industrial applications. Commonly observed phases of polycrystalline tin oxide include rutile structure SnO_2 and litharge structure SnO in crystalline forms corresponding to tin oxidation states +4 and +2. The fact that different cation oxidation states are possible implies that a variety of nonstoichiometric structures (SnO_x, $x < 2$ and SnO_2/SnO interfaces) may be formed [1–3], with lower formation energy (less stable) than the sum of ideal separated SnO and SnO_2 crystals. Experimental observations suggest that at slightly elevated temperatures in the absence of excess oxygen, nonstoichiometric crystallites with composition at or near tin sesquioxide Sn_2O_3, can form, as will be discussed later.

It is well-known that when annealed in oxygen rich environment, SnO phase transforms to SnO_2 phase within and above the temperature range 600–900 K [5–7]. Such transformations

[1] Author to whom any correspondence should be addressed.

0965-0393/04/010033+09$30.00

can occur by a modest displacement of tin atoms in tin matrix [7, 8]. In experiments, it has turned out that well-defined solid intermediate phases also exist [2, 5–7, 9] and corresponding cell parameters have been determined by x-ray diffraction [10]. In these experiments, tin monoxide disproportionates (is oxidized and reduced) with SnO_2 at temperatures above 600 K producing Sn_2O_3 in addition to metallic tin and SnO_2 [5, 10]. More recently, also at the interface of SnO_2/SiO_x [11] and on the surface of Fe_2O_3 [12], formation of related films of tin oxides have been suggested. It should be noticed that the diffraction measurements do not always provide definite information and can be interfered by presence of H_2O [13].

On the other hand, it is also known that mainly thin films and small crystallites may adopt Sn_2O_3 phases, which dissociate slowly [4]. In the case of gas sensor applications, for instance, such crystallites are important. Of course, some structures with the composition Sn_2O_3 can also be understood as a special cases of SnO_2/SnO interfaces. Simple models of interface structures between SnO_2 and SnO crystals have been introduced associated with amorphous and nanoparticle tin oxide [6,8,14,15]. In these structures high-resolution electron microscopy (HREM) has indicated that $SnO_2(101)$ layers are usually alongside SnO(001) layers [6, 15].

To investigate these materials, we present a theoretical survey of possibilities for ordered crystalline compounds and interfaces limited to the composition Sn_2O_3. It is important to restrict the composition to compare straightforwardly different interfaces with each other, with perfect SnO and SnO_2 crystals and with other possible Sn_2O_3 crystal structures. It has been noticed that there are also some other possibilities for formation of ordered tin oxide crystals including orthorhombic SnO phase [2,5,8,16]. In comparison to related metal oxides, decomposition of PbO_2 and oxidation of PbO to the intermediate oxides has been a subject of active research [16].

This paper is organized as follows. In section 2 the calculation method is described followed by the discussion of geometries in sections 3–5. In section 6 discussion and conclusions are presented.

2. Methods

Electronic structures and energetics of the Sn_2O_3 structures are calculated using first principles density functional method and plane wave basis combined with ultra-soft pseudopotentials (CASTEP/CETEP code) [17, 18]. Oxygen atoms are described by six valence electrons and tin atoms by four electrons plus the corresponding pseudopotential ion cores. The plane wave cutoff is 400 eV. Electronic exchange and correlation are taken into account with the generalized-gradient approximation (GGA) [19]. A few optimization experiments were performed also by using local density approximation (LDA) [20]. To sample the Brillouin zone, the number of symmetrized Monkhorst–Pack k-points [21] varies between 4 and 20 depending on the size of the cell. For crystalline SnO_2 and SnO, experimentally known cell parameters are reproduced with an accuracy of 0.5–1.8%. For heats of formation the agreement with less accurate experimental values is of the order of 3%. For bulk moduli the accuracy is better than 10%.

The structures of tin sesquioxide were generated based on geometry optimization including variation of cell parameters. The convergence criteria for geometry optimizations, in terms of tolerance for the root mean square force on atoms was 0.005 eV $Å^{-1}$ and for the root mean value of the stress tensor 0.07 GPa. In the case of the largest structure (shown in figure 3), the latter criteria was reduced (to 0.3 GPa), which was reasonable to save computational resources, in addition high stability of the well-formed structure was achieved (see later). Space-groups of resulting crystal structures [22] were determined by utilizing Cerius^2 Crystal Builder (by Accelrys Inc.), with a tolerance (for two atoms to be equivalent by symmetry) of 0.1 Å.

To provide information of the properties at nonzero pressure and temperature conditions, rough estimates for bulk modulus and free energy were evaluated. To determine the cell volume V as a function of hydrostatic pressure P, crystals were influenced by external hydrostatic pressure and total enthalpy ($E + PV$) of crystals was minimized. Bulk modulus ($-V(\partial P/\partial V)$) was evaluated from the pressure volume function by fitting a polynomial to the data. Temperature contribution to the free energy is straightforwardly obtained based on the Debye approximation, once the Debye temperature Θ_D is known [25–27]. As a first approximation, Θ_D is expressed in terms of bulk modulus B (in Mbar), density ρ (in g cm^{-3}) and molecular mass M (in atomic mass units) as $1550B^{1/2}\rho^{-1/6}(p/M)^{1/3}$, where p is the number of atoms in the cell [25,28] ($p = 5$ for Sn_2O_3). In the case of SnO_2 this equation gives Θ_D of 450 K, to be compared with experimental value 570 K [29]. For SnO, similar analysis gives Θ_D of order 200 K, due to its low bulk modulus. However, it should be noticed that such estimates are better defined for more isotropic nonlayered geometries.

3. SnO_2, SnO and SnO_2 + SnO reference system

The unit cell of the well-known rutile structure SnO_2 crystal, can be viewed to be constructed of SnO_6 structure in a geometry corresponding to almost ideal octahedra at whose centre Sn^{4+} type of ion is located. These octahedra are arranged to share two common edges. Tin oxide SnO crystal with litharge structure is instead a layered crystal composed of SnO_4 tetrahedron units. Its tin ions are designated as Sn^{2+} and are associated with a lone pair electron density pointing away from the layer. The formation of these structures can be explained in a substantial part by Pauling's arguments for stable ionic systems [30]. They state that the presence of shared edges, and especially, shared faces in a coordinated structure (polyhedron) decrease the stability. The decrease in stability arises from interaction between cations [30].

A natural reference system to Sn_2O_3 structures is a sum of ideal and independent SnO_2 and SnO crystals (SnO_2 + SnO), which allows a direct comparison of total energy to Sn_2O_3. An alternative reference system, which was found to be less stable, would be a combination of SnO and oxygen gas ($2SnO + 0.5O_2$). In this case, the contribution of the oxygen depends on the oxygen pressure, similarly as discussed in [31]. Possible structures could have also been compared to the sum of independent metallic tin and SnO_2 crystals ($1.5SnO_2 + 0.5Sn$). This system was actually found to be slightly more stable than SnO_2 + SnO, by 0.1 eV/Sn_2O_3. This result is consistent with the production of metallic tin during disproportionation, as indicated above. However, this reference was not chosen, since it was preferred to compare nonmetallic materials with one another.

4. Sn_2O_3 crystals

Attempts to equilibrate stable Sn_2O_3 structures were focused on crystals with small unit cell (size of order $4 \times 8 \times 6$ Å). Initially, different known metal oxide crystal geometries were used. To obtain other starting geometries, additional procedures included forced symmetrization and symmetry reduction, scaling and fixing of cell parameters and different removals and attachments of oxygen atoms to tin atoms.

It seems apparent that stable layered crystals with Sn_2O_3 composition can be constructed by adding oxygen atoms between separated layers of SnO crystal. Alternatively, one can separate a layer from SnO_2 crystal, remove oxygens from the surface of the layer and build up a layered Sn_2O_3 crystal. Such a layered crystal corresponding to $SnO_2(101)$ surface slabs or layers (shown in figure 1(*a*)) is noticed to be associated with considerable stability. This kind

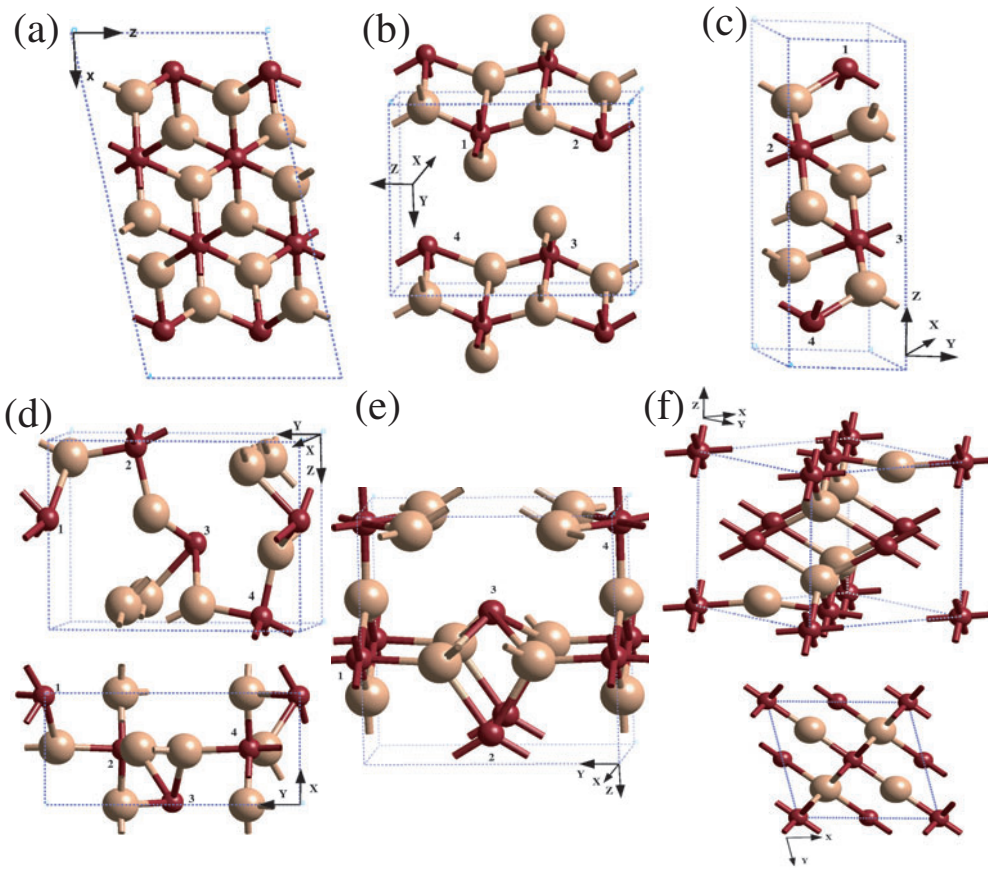

Figure 1. Possible structures of Sn_2O_3 crystals. Light balls denote oxygen atoms and the dark ones denote tin atoms. Primitive cells are shown: (*a*) layered crystal with oxygen vacancies at (101) plane of SnO_2; (*b*) layered crystal with $P2_1/m$ symmetry. The bond lengths range between 2.0 and 2.2 Å; (*c*) layered crystal with $P2_1/m$ symmetry. In contrast to (*b*) the structure is labelled here as Sn_2O_3 $P2_1/m^*$; (*d*) structure with symmetry $P2_1$; (*e*) structure with symmetry Pm; (*f*) structure with symmetry $Cmma$. The bond lengths range between 1.9 and 2.3 Å.

of a geometry is related to the crystallographic shear plane defects [1,3,33]. The total energy of this structure is about equal to the sum of that of independent SnO and SnO_2 crystals. A more detailed comparison suggests that the GGA total energy of this crystal is below the $SnO+SnO_2$ reference by 0.02 eV/Sn_2O_3. In contrast, if the three calculations (for SnO, SnO_2 and Sn_2O_3) are performed by using LDA, the SnO and SnO_2 references are more stable by 0.1 eV/Sn_2O_3. To find a contribution of the associated vacuum layer, its thickness was increased (from 2.65 to 12 Å) so that the interaction across it becomes minimal. After geometry optimization, it was found that the total energy is increased only by 70 meV/Sn_2O_3. Thus, the interaction across the vacuum is weak and the stability of the structure in figure 1(*a*) is contributed largely by its oxygen deficient SnO_2(101) surface slab. Cell parameters of this geometry, which is labelled by Sn_2O_3(101), are listed in table 1.

A possibility of the SnO structure crystals containing additional oxygen has been indicated in samples made by evaporating SnO and SnO_2 powders [34]. This kind of Sn_2O_3 crystal lattice, belonging to the $P2_1/m$ space group, is shown in figure 1(*b*). When this structure was squeezed, so that adjacent layers interact strongly, another Sn_2O_3 structure with considerably

Table 1. Cell parameters, mass densities (ρ) and total energies (E) per Sn_2O_3 unit at 0 K. The total energy is with reference to the sum of SnO and SnO_2 (SnO + SnO_2). Measured cell parameters of Sn_2O_3 and Sn_3O_4 crystals (Exp.) and corresponding parameters of the SnO/SnO_2 interface are also listed. The densities are evaluated from the cell parameters.

	a (Å)	b (Å)	c (Å)	α	β	γ	E (eV)	ρ (g cm^{-3})
Exp. [10] $2Sn_2O_3$	3.71	8.18	5.46	90	92.3	93.8		5.7
Exp. [2] Sn_3O_4	4.86	8.20	5.88	93.0	91	93.2		6.0
Sn_2O_3(101) (figure 1(*a*))	10.71	4.76	5.74	90	77.8	90	0.0	6.6
$P2_1/m$ (11) (figure 1(*b*))	3.17	5.98	8.08	89.6	90.0	89.7	0.7	6.2
$P2_1/m^*$ (11) (figure 1(*c*))	4.86	3.18	10.3	90	105	90	0.2	6.2
$P2_1$ (4) (figure 1(*d*))	3.57	7.74	5.31	90	89.5	90	1.2	6.5
Pm (6) (figure 1(*e*))	3.07	6.41	6.74	90	90	90.1	0.6	7.2
$Cmma$ (67) (figure 1(*f*))	4.89	4.89	5.44	90	90	76.6	1.4	7.5
SnO_2(100)/SnO(100)	47.2	4.72	3.18	90	90	90	0.3	6.7
SnO_2(101)/SnO(001)	4.79	5.67	25.5	112	89.8	90	0.1	5.9
SnO	3.74	3.74	4.75	90	90	90		6.7
SnO_2	4.72	4.72	3.14	90	90	90		7.2
SnO + SnO_2							0.0	7.0

increased stability is formed. The structure, illustrated in figure 1(*c*), remains layered and belongs to the $P2_1/m$ crystallographic space group. We will thus label the structure as Sn_2O_3 $P2_1/m^*$. The structure is composed of SnO_6 and SnO_3 polyhedra units and the total energy per Sn_2O_3 unit is 0.2 eV above the reference. Atoms of this special structure are at positions: Sn_1 1.29, 2.38, 3.62; Sn_2 −1.56, 2.38, 8.62; O_1 2.09, 0.79, 4.65; O_2 −0.67, 0.79, 7.65; O_3 1.74, 2.38, 7.26 Å.

A primitive unit cell of a nonlayered Sn_2O_3 crystal structure whose cell parameters were found to be in close agreement with the experimental parameters of [10] is illustrated in figure 1(*d*). The agreement of the cell parameters is better than 6% (see table 1). The lattice is composed of SnO_5 and SnO_4 polyhedra and the space group to which the lattice belongs is $P2_1$. This structure is not as stable as those mentioned above, with the total energy of Sn_2O_3 unit 1.2 eV above the reference. However, a low value of the evaluated bulk modulus (100 GPa) of this crystal can, in principle, be attributed to its formation in the case of a strained layer [35]. Atoms of this structure are at positions: Sn_1 0.11, 3.87, 3.10; Sn_2 1.77, 5.38, 0.26; O_1 1.85, 7.38, 0.59; O_2 1.80, 4.90, 2.15; O_3 0.00, 1.60, 0.69 Å. In attempts to reach an agreement with the experimental parameters, crystals with slightly improved stability but with cell parameters differing by about 10% from the experimental values were constructed by starting from Perovskite-type structures (e.g. $SrTiO_3$).

A primitive cell of a relatively stable and compact nonlayered Sn_2O_3 crystal structure is illustrated in figure 1(*e*) corresponding to Pm symmetry. The structure is constructed by removing oxygen atoms from SnO_2 crystal. The cell is again composed of SnO_6 and SnO_4 polyhedra elements. Tin atoms are at positions: Sn_1 −0.01, 3.21, 5.91; Sn_2 0.00, 0.05, 3.84; Sn_3 1.52, 3.29, 2.87; Sn_4 1.53, 0.01, 0.43 Å. This structure has a bulk modulus of 150 GPa. Relatively dense space filling and high value of bulk modulus 170 GPa, was obtained for Sn_2O_3 crystal shown in figure 1(*f*) with symmetry $Cmma$. The structure is also composed of SnO_6 and SnO_4 polyhedra, and the tin atoms are at face centred positions of the cell faces. The $Cmma$ structure is the least stable of those considered here with the total energy of Sn_2O_3 unit 1.4 eV above the reference. Its formation can, in principle, be favoured at high pressure conditions due to associated dense space filling [36].

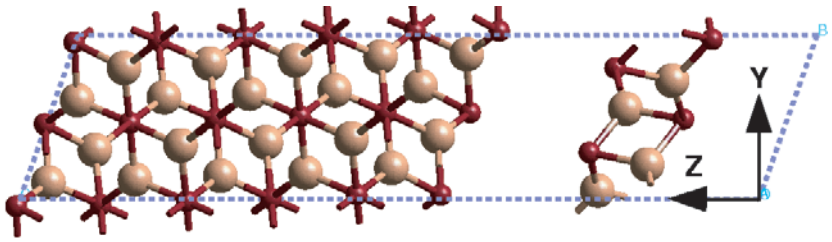

Figure 2. Sn_2O_3 structure consisting of separated SnO_2 (at left) and SnO (at right) phases. Their surface orientations correspond to $SnO_2(101)$/SnO(001) interfaces.

Some estimates of the contribution due to temperature and entropy dependent contributions concerning Sn_2O_3 crystals can be straightforwardly made. These contributions can be assumed not to be very significant at the relatively low temperatures where the SnO_x phases are observed. By comparing temperature contributions, using the Debye approximation [25], it was noticed that the free energy of Sn_2O_3 $P2_1$ crystal is significantly reduced, due to its lowest Θ_D (295 K). For crystals with symmetry Pm and $Cmma$, Θ_D are 355 K and 375 K, respectively. The values of Θ_D around 300 K at temperature 600 K can amount to about 0.15 eV decrease of the free energy. However, estimated Θ_D for SnO is lower (200 K) amounting to larger free energy decrease in the case of $SnO+SnO_2$. Thus, the ordering of stability of the different (nonlayered) crystals is not assumed to be changed by including free energy contributions.

5. SnO_2/SnO interfaces

Stability of the Sn_2O_3 structures, and especially that depicted in figure 1(*a*), is quite remarkable. However, interfaces between SnO/SnO_2 crystals can be important alternatives to these systems. Two such periodic structures, restricted to Sn_2O_3 composition, are considered here. Their surface orientations are $SnO_2(101)$/SnO(001) and $SnO_2(100)$/SnO(100), which correspond to experimental measurements [6, 14].

The optimized structure with $SnO_2(101)$/SnO(001) interfaces is shown in figure 2. Similarly with the structure of figure 1(*a*), it is composed of (slightly deformed) oxygen deficient (101) SnO_2 surface alongside the SnO layer. There is a vacuum of thickness 4.5 Å between the SnO and SnO_2 types of structure. It can be expected that the system has a considerable stability and ability to relax quite freely due to the weakly bound SnO/SnO_2 interfaces. Cell parameters of the geometry are listed in table 1.

The optimized structure of the other interface structure including $SnO_2(100)$/SnO(100) interfaces is shown in figure 3. It is constructed by attaching cell faces after which tin ions with four oxygen neighbours forms at the interface. Due to the lack of reflection symmetry, the shown unit cell is the shortest in the [100] direction. The SnO parts of the interfaces become compressed by 15% along z-direction of figure 3 with respect to SnO crystal. Other strains with respect to SnO and SnO_2 crystals were less than 2%.

It is of interest to compare total energies of interfacial Sn_2O_3 structures to the combined SnO and SnO_2 crystals including also an estimate of their interface energy. The system of figure 2 has an interface energy of 0.15 J m^{-2} per interface. This was evaluated by comparing the total energy of the structure to the sum of total energies of SnO and SnO_2 crystals. The formation energy is 60 meV per Sn_2O_3 unit. The stability of this structure can be largely explained by its structural similarity with the geometry of figure 1(*a*). A larger interface energy, 0.8 J m^{-2} per $SnO_2(100)$/SnO(100) interface, is obtained in the case of figure 3. This

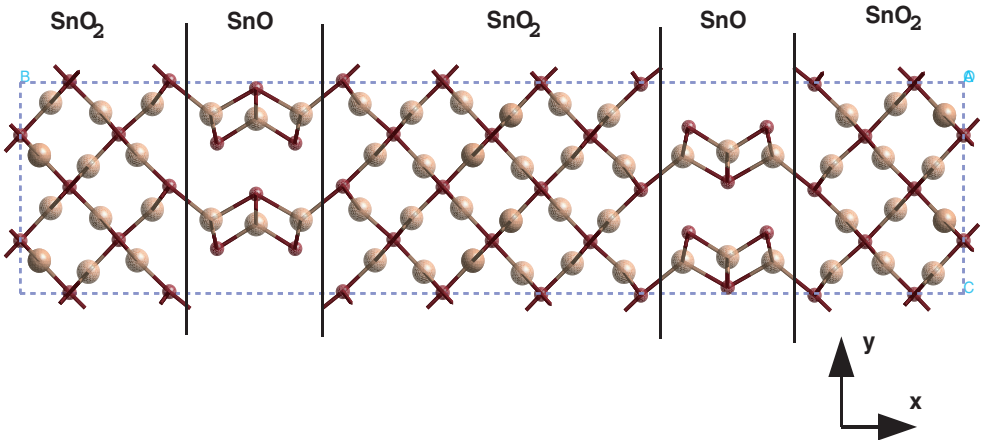

Figure 3. Sn_2O_3 structure consisting of $SnO_2(100)$/SnO(100) interfaces. For illustration, the cell is doubled along y-direction.

corresponds to a formation energy of 75 meV per Sn_2O_3 unit with respect to the reference system. If there are four interfaces in the cell (as in figure 3), the formation energy is 0.3 eV. For comparison, the estimated interface energies are less than the calculated surface energies of SnO_2 crystal, which exceed 1 J m^{-2} [32].

6. Discussions and conclusions

Density functional calculations provide evidence for existence of different ordered nonstoichiometric crystalline structures of tin oxide. Layered Sn_2O_3 crystals and SnO/SnO_2 interface crystals (figures 1(*a*) and 2) were found to be among the most stable structures. A common feature of these systems is a similar oxygen deficient $SnO_2(101)$ surface immersed inside the structures. It seems likely that structures having oxygen deficiency with respect to bulk SnO_2 may evolve by forming these structures. Unfortunately, the structure of figure 1(*a*) may not be easily observed in HREM measurements, since the distance between its (101) tin planes varies only between 2.61 and 2.65 Å.

It is also possible that at some special environments and conditions other less stable systems may stabilize, or serve as some metastable transition structures. These possibilities refer to externally applied pressure, elevated temperatures, strained nanocrystals inside a host material, strained interface structures, etc. For instance, in case of nearly perfect SnO crystals, excess oxygen can exist between its SnO layers, as in the case of figure 1(*b*). Such structure may easily transform and stabilize to other structures like those of figures 1(*a*) and (*c*) depending on temperature and pressure. The soft structures like that of figure 1(*d*), may have significance in very small grains, which are usually considerably strained. Charging of the structures may also have an influence by changing the lattice constants [37]. Assuming that layered Sn_2O_3 geometries are readily obtainable, the properties of such materials also become influenced significantly by associated microstructure. This is analogous to the case of layered materials like graphite, which can exist in states ranging from crystalline to amorphous.

In conclusion, most stable structures were found to be based largely on the rutile structure of SnO_2, and to a less extent on litharge structure of SnO crystals. The Sn_2O_3 structures considered here have 0.0–1.4 eV smaller heat of formation than the sum of heats of formation

of SnO and SnO_2, thus being less stable. The SnO/SnO_2 interface considered has an interface energy of 0.15 J m^{-2} in the case of SnO_2(101)/SnO(001) surface orientations, and 0.8 J m^{-2} in the case of SnO_2(100)/SnO(100) surface orientation. It is predicted that the nonstoichiometric Sn_2O_3 composition tends to evolve to form layered oxygen deficient SnO_2(101) structures. A related structure, where also SnO phase with SnO_2(101)/SnO(001) interface(s) are included, provides a slightly less stable alternative. This system may be able to adapt easily to different compositions and environments due to the weakly bound SnO/SnO_2 interfaces and SnO layers.

Acknowledgments

We are grateful for the support from the Graduate school of functional surfaces and by MECA project (both funded by The Academy of Finland). We also acknowledge computational resources of the Center for Scientific Computing (CSC, Project TTKK-4585) Espoo, Finland. This work was also supported by EC in the frame of INTAS Program (INTAS-2001-0009).

References

[1] Sørensen O T 1981 *Nonstoichiometric Oxides* (London: Academic) p 2
[2] Lawson F 1967 *Nature* **215** 955
[3] Zheng J G, Pan X, Schweizer M, Weimar U, Göpel W and Rühle M 1996 *Phil. Mag. Lett.* **73** 93
[4] Martel A, Caballero-Briones F, Bartolo-Pérez P, Iribarren A, Castro-Rodríguez R, Zapata-Navarro A and Peña J L 2001 *Surf. Coat. Technol.* **148** 103
[5] Choi W K, Sung H, Kim K H, Cho J S, Choi S C, Jung H-J, Koh S K, Lee C M and Jeong K 1997 *J. Mater. Sci. Lett.* **16** 1551
[6] Pan X Q and Fu L 2001 *J. Appl. Phys.* **89** 6048
[7] Geurts J, Rau S, Richter W and Schmitte F J 1984 *Thin Solid Films* **121** 217
[8] Kaito C and Saito Y 1986 *J. Cryst. Growth* **79** 403
[9] Madhusudhana Reddy M R, Jawalekar S R and Chandorkar A N 1989 *Thin Solid Films* **169** 117
[10] Murken Von G and Trömel M 1973 *Z. Anorg. Allg. Chem.* **897** 117
[11] Alfonso C, Charai A, Armigliato A and Narducci D 1996 *Appl. Phys. Lett.* **68** 1207
[12] Ichiba S, Oshita H and Sakai H 1990 *Chem. Lett.* 437
[13] Srinivasa Murty N and Jawalker S R 1983 *Thin Solid Films* **100** 219
[14] Tsunekawa S, Kang J, Asami K, Kawazoe Y and Kasuya A 2002 *Appl. Surf. Sci.* **201** 69
[15] Kobayashi T, Kimura Y, Suzuki H, Sato T, Tanigaki T, Saito Y and Kaito C 2002 *J. Cryst. Growth* **243** 143
[16] Wells A F 1984 *Structural Inorganic Chemistry* (Oxford: Clarendon)
[17] Milman V, Winkler B, White J A, Pickard C J, Payne M C, Akhmatskaya E V and Nobes R H 2000 *Int. J. Quant. Chem.* **77** 895
[18] Vanderbilt D 1990 *Phys. Rev.* B **41** 7892
[19] Perdew J P and Wang Y 1992 *Phys. Rev.* B **46** 6671
[20] Perdew J P and Zunger A 1981 *Phys. Rev.* B **23** 5048
[21] Monkhorst H J and Pack J D 1976 *Phys. Rev.* B **13** 5188
[22] Hahn T 1984 *International Tables for Crystallography: Volume A. Space-Group Symmetry* (Dordrecht: Kluwer)
[23] Pannetier J and Denes G 1980 *Acta Crystallogr.* B **36** 2763
[24] Wagman D D, Evans W H, Parker V B, Schumm R H, Halow I, Bailey S M, Churney K L and Nuttall R L 1981 *The NBS Tales of Chemical Thermodynamic Properties* (Washington, DC: National Bureau of Standards)
[25] Moruzzi V L, Janak J F and Schwarz K 1988 *Phys. Rev.* B **37** 790
[26] Söderlind P 1994 *PhD Thesis* (Uppsala: Acta Universitatis)
[27] Mason W P 1965 *Physical Acoustics* vol III-B (New York: Academic)
[28] Anderson O L 1998 *Am. Miner.* **83** 23
[29] Tuerkes P, Pluntke Ch and Helbig R 1980 *J. Phys. C: Condens. Matter* **13** 4941
[30] Pauling L 1960 *The Nature of the Chemical Bond* (New York: Cornell University Press)
[31] Reuter K and Scheffler M 2003 *Phys. Rev.* B **65** 035406
[32] Mäki-Jaskari M A and Rantala T T 2001 *Phys. Rev.* B **64** 075407

[33] Nörenberg H, Tanner R E, Schierbaum K D, Fischer S and Briggs G A D 1998 *Surf. Sci.* **396** 52
[34] Yamazaki T, Mizutani U and Iwama Y 1982 *Japan. J. Appl. Phys.* **21** 440
[35] Cabrera N and Mott N F 1948 *Rep. Prog. Phys.* **12** 163
[36] Verma A R and Krishna P 1966 *Polymorphism and Polytypism in Crystals* (New York: Wiley)
[37] Albaret T, Finocchi F and Noguera C 2000 *J. Chem. Phys.* **113** 2238